Soft Matter

PAPER

The piezoresponse force microscopy investigation of self-polarization alignment in poly(vinylidene fluoride-*co*-trifluoroethylene) ultrathin films

Moonkyu Park,[a] Yoon-Young Choi,[a] Jiyoon Kim,[a] Jongin Hong,*[b] Han Wook Song,[c] Tae-Hyun Sung[d] and Kwangsoo No*[a]

We report the self-polarization alignment without external poling in spin-coated poly(vinylidene fluoride-*co*-trifluoroethylene), P(VDF-TrFE), thin films on transparent and flexible substrates. Piezoresponse force microscopy (PFM) allows the quantitative analysis of preferentially aligned polarization in the ferroelectric thin films. We found that as-received P(VDF-TrFE) thin films on transparent poly(3,4-ethylenedioxythiophene):poly(4-styrenesulfonate) (PEDOT:PSS) electrodes showed stronger self-polarization alignment than those on indium-tin oxide (ITO) electrodes. The relative ratios for the aligned polarization per unit volume on PEDOT:PSS and ITO electrodes were 18.6% and 4%, respectively.

Introduction

Organic ferroelectric materials have attracted attention for their emerging applications in organic electronics, radio-frequency identification (RFID) tags and energy harvesters.[1–3] Most current studies are focused on PVDF [polyvinylidene fluoride; $(CH_2CF_2)_n$] and its copolymer P(VDF-TrFE) [poly(vinylidene fluoride-*co*-trifluoroethylene), $(CH_2CF_2)_n$-$(CHFCF_2)_m$] because of a relatively large remnant polarization, a short switching time and a good thermal stability.[4,5] Unfortunately, PVDF needs additional steps such as mechanical stretching and/or electric poling to obtain its ferroelectricity. These laborious steps can be avoided by chemical modification through copolymerization with TrFE that induces an all *trans* stereochemical conformation that aligns the direction of the dipole moments. To date, a number of efforts have been made to improve the ferroelectric properties of P(VDF-TrFE) ultrathin films[6–12] and to characterize their nanoscale properties by piezoresponse force microscopy (PFM).[13–18] For example, Ducharme and co-workers have demonstrated ultrathin and high quality crystalline P(VDF-TrFE) films on various substrates by a Langmuir–Blodgett (LB) technique.[6,7] Xu *et al.* reported that the usage of conductive polymer electrodes would result in an increase in remnant polarization and a decrease in the polarization

switching time of the P(VDF-TrFE) thin films.[9,10] Their fatigue endurance for long operation was also improved because the conductive polymer electrodes supplied free charges to compensate and stabilize dipoles in the films. Recently, Kusuma *et al.* introduced the incorporation of gold nanoparticles into P(VDF-TrFE) films to enhance ferroelectric switching characteristics.[12] Meanwhile, the PFM measurements have been performed to probe the static and dynamic properties of P(VDF-TrFE) films and nanostructures at nanoscale.[13–18] Rodriguez *et al.* manipulated ferroelectric domains with polarization control of a resolution below 50 nm and imaged single-domain regions with an imaging resolution below 5 nm in the ferroelectric LB film on graphite.[13] They also reported the inhomogeneous polarization relaxation within P(VDF-TrFE) nanomesa using time-resolved piezoresponse force spectroscopy (TR-PFS).[14] Kim *et al.* investigated the nanoscale domain growth dynamics in the spin-coated P(VDF-TrFE) film on a Au/Cr/SiO_2/Si substrate.[15] He also suggested that its switching behaviour would be dominated by domain nucleation. Recently, Sharma *et al.* carried out resonance-enhanced PFM investigation with sub-10 nm lateral resolution to delineate polarization distribution and determine local switching behaviour in P(VDF-TrFE) nanostructures on highly doped silicon substrates.[18] Even though PFM made a crucial contribution toward the fundamental studies of ferroelectric polarization in PVDF-TrFE, relatively few PFM studies have been devoted to analyzing spin-cast ultrathin films on flexible substrates.

On the other hand, organic electronic devices integrated with flexible and transparent substrates have been envisioned as the next generation of ultralow-cost, lightweight and stretchable devices, which will be a viable alternative to conventional silicon-based electronic devices.[19,20] Examples are touch screens, flexible displays, sensory skins, structural health monitors and wearable

[a] Department of Materials Science and Engineering, KAIST, Daejeon, 305-701, Korea. E-mail: ksno@kaist.ac.kr; Fax: +82 42 350 3310; Tel: +82 42 350 4156
[b] Department of Chemistry, Chung-Ang University, Seoul, 156-756, Korea. E-mail: hongj@cau.ac.kr; Fax: +82 2 825 4736; Tel: +82 2 820 5869
[c] Group of Standard and Basis Metrology, Korea Research Institute of Standard and Science, Daejeon, 305–340, Korea
[d] Department of Electrical Engineering, Hanyang University, 17 Haengdang-dong, Seongdongu-gu, Seoul, 133-791, Korea

communication devices. Currently, indium tin oxide (ITO) is the market standard of flexible transparent conductors for these applications. However, ITO is not an ideal material due to both technical and economical reasons: indium is expensive and scarce. Its preparation requires high-temperature processing for complete crystallization. The crystalline films may fracture when stretched or bent. In particular, release of indium and oxygen into a functional organic layer should be avoided. Instead of ITO, poly(3,4-ethylenedioxythiophene) (PEDOT) doped with poly(4-styrenesulfonate) (PSS) is considered as a promising organic-based electrode. To date, PEDOT:PSS has been extensively utilized as either a transparent electrode or a hole injection layer in most organic devices including light-emitting devices and photovoltaic devices.[21,22] Regrettably, ferroelectric polymers on ITO and PEDOT:PSS have not been much investigated so far even though they are important for low-cost data storage and electromechanical applications. Very recently, we investigated the effect of electrode materials on nanoscale ferroelectric properties in terms of interfacial interaction between P(VDF-TrFE) and bottom electrode layers.[17] However, we did pay a little attention to a significant polarization (called self-polarization) in the P(VDF-TrFE) films, which is not typically observed in ferroelectric bulk polymers. Interestingly, the self-polarization is advantageous to pyroelectric, piezoelectric and ferroelectric applications since the subsequent poling procedure (i.e. a strong electric field at elevated temperatures) can be avoided. It is also hard to uniformly polarize a large number of electronic elements by conventional poling techniques. Accordingly, we describe the quantitative evaluation of self-polarization from PFM measurements in the P(VDF-TrFE) films on different electrode materials. To our knowledge, no study of such quantitative PFM analysis has been undertaken. Additionally, discussion in this article will centre around finding possible mechanisms of the self-polarization in the P(VDF-TrFE) ultra-thin films.

Experimental

Materials

Polyethylene naphthalate (PEN) was selected as a transparent flexible substrate because of its higher glass transition temperature and hardness when compared to polyethylene terephthalate (PET). 250 nm-thick ITO-coated PEN sheets were purchased from ISC Co., Korea. An aqueous dispersion of PEDOT:PSS (Clevios™ PH 500, H.C. Starck, GmbH, Germany) doped with 5% dimethyl sulfoxide was spun on oxygen plasma-treated PEN substrates at 1500 rpm for 20 s followed by annealing at 125 °C for 30 min, resulting in 60 nm-thick PEDOT:PSS films. For a ferroelectric layer, 1 wt% P(VDF-TrFE) solution was prepared by dissolving P(VDF-TrFE) powders in a molar ratio of 75/25 in methyl ethyl ketone (MEK) and then was spin-coated at a spin rate of 5000 rpm for 20 s on the substrates mentioned above. Subsequently, the samples were annealed at 110 °C for 2 h on a hot plate. The final thickness of P(VDF-TrFE) films on ITO and PEDOT:PSS was about 20 nm. In addition, P(VDF-TrFE) films on Au/Si substrates were also prepared at the same spin-coating condition as reference for quantitative PFM measurements.

Methods

Electrical properties of ITO and PEDOT:PSS were investigated by using a 4-point probe system (SR1000N, AIT Co., Ltd.) and a Hall measurement system based on the van der Pauw method (Ecopia HMS-3000, Bridge Technology). They are summarized in Table 1. PFM measurements were performed, under ambient conditions, using a commercial atomic force microscope (XE-100, Park systems, Korea) equipped with lock-in amplifier (SR830, Stanford Research System). A controlled modulation voltage of 0.8 V_{rms} at 17 kHz was applied to the P(VDF-TrFE) thin films to measure their electromechanical response. The usage of a Pt-coated Si tip (Micromasch, spring constant k ≈ 6.0 N m^{-1}) allowed for measuring local electrical and topological properties of the ferroelectric polymers both simultaneously and independently. Importantly, piezoelectric hysteresis loop measurements were conducted on P(VDF-TrFE) films to determine a favoured polarization state during fabrication. To obtain a single hysteresis loop at each position, we used a continuous dc mode that consists of measuring the induced piezoelectric vibration while continuously increasing and decreasing the additional dc voltage. The dc voltage was applied to the bottom electrode (sequence 0 V → +10 V → 0 V → −10 V → 0 V) and superimposed onto the small ac modulation voltage applied to the tip. Each voltage step was 400 mV for 200 ms. We calibrated photodiode voltage outputs of the piezoelectric vibration using force–distance measurements to convert them to effective d_{33} piezoresponse (pm V^{-1}). 10 positions of each experimental case were randomly selected and their hysteresis loops were averaged.

Results and discussion

Fig. 1 shows topological, PFM amplitude and PFM phase images of the P(VDF-TrFE) thin films coated on ITO and PEDOT:PSS electrodes. In the PFM measurements, an amplitude signal indicates a longitudinal piezoelectric coefficient (or deviation of polarization from a surface normal), whilst a phase signal indicates the polarization direction.[16,17] In our PFM phase images, a dark contrast indicates the downward polarization direction whilst bright contrast indicates upward polarization. Interestingly, as-received P(VDF-TrFE) thin films on both ITO and PEDOT:PSS electrodes showed uniform dark contrast in the phase images. However, the amplitude value of P(VDF-TrFE) film on PEDOT:PSS electrode was higher than that on ITO electrode. The average amplitude values of voltage for P(VDF-TrFE) films over the scanned area were 426.7 ± 68.2 mV and 235.9 ± 46.4 mV for the PEDOT:PSS electrode and ITO electrode, respectively. These results indicate that electric dipoles in the virgin P(VDF-TrFE) films were self-aligned in the direction from surface to the bottom electrode. It should be noted that PEDOT:PSS allowed for better self-polarization alignment to the surface normal when compared to ITO. For quantitative evaluation of the initial piezoelectric response, local piezoresponse hysteresis loops were used. The piezoelectric response is apparently proportional to both switchable and non-switchable polarizations in this method. The initial amount of self-polarization, P_{self}, can be determined through the first measured PFM hysteresis loop since it reflects the initial state of polarizations in the ferroelectric films.

Table 1 Surface roughness and electrical properties of transparent and flexible substrates

Substrate	Surface roughness (nm)	Sheet resistance ($\Omega/\square$)	Carrier Conc. (cm^{-3})	Mobility (cm^2 V^{-1} s^{-1})
ITO/PEN	0.44 ± 0.01	13.39 ± 0.022	9.833×10^{20}	2.392×10^{1}
PEDOT:PSS/PEN	1.33 ± 0.04	262.7 ± 0.294	7.375×10^{17}	1.397×10^{3}
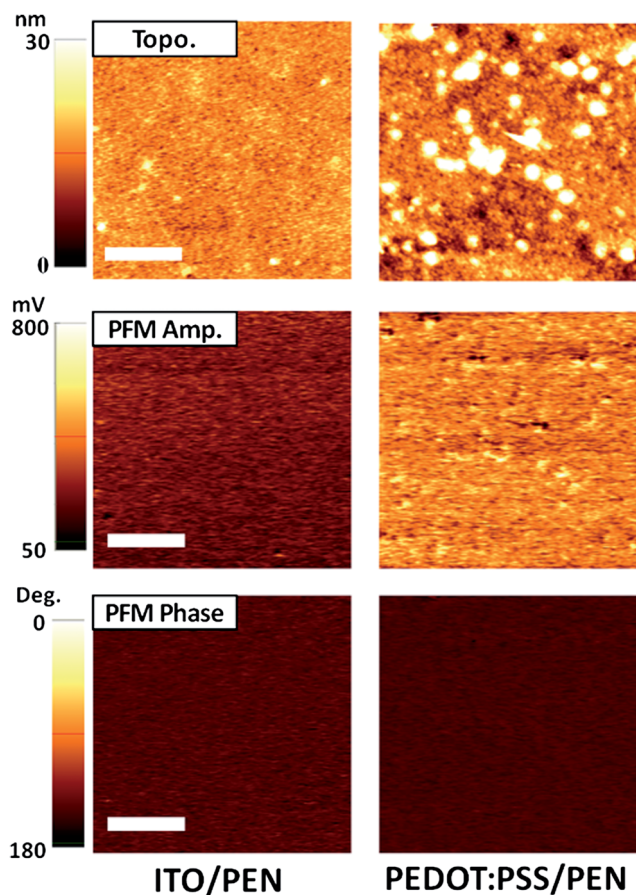
Fig. 1 (Upper) Topography, (middle) PFM amplitude and (lower) PFM phase images of P(VDF-TrFE) thin films coated on (left) ITO/PEN and (right) PEDOT:PSS/PEN substrates. Scale bars represent 3 μm.

The PFM investigation of self-polarization alignment is as follows. Firstly, we obtained each local hysteresis loop from three different regions (virgin state, poling of −5 V and poling of +5 V) in P(VDF-TrFE) films on Au/Si substrates to determine the polarization direction. The poling process was performed by applying external voltage to the conductive AFM tip over a scan area. In Fig. 2(b) and (c), PFM amplitude and phase images showed that the polarization directions of regions poled with −5 V and +5 V were upward (bright contrast in the PFM phase image) and downward (dark contrast in the PFM phase image), respectively. Fig. 2(d) shows the first measured hysteresis loops of the three different regions. We observed that the start point of each loop (marked as red circles) was placed at a different position. The initial point obtained from the region poled with −5 V was located at a negative value on y-axis that indicates upward polarization and *vice versa*. Interestingly, a positive value from the virgin state in the firstly measured hysteresis loop was recorded and this means the presence of *self-polarization*,

a remnant polarization in the thin films without any previous poling treatment. Fig. 2(e) shows hysteresis loops that were secondly measured at the same positions in the three different regions. All the loops were almost identical and continuous in contrast to those first measured. Accordingly, we would easily determine self-polarization vector and its amount by carefully monitoring the first PFM hysteresis loop.

We also investigated how the poling voltage would affect the amount of deliberately aligned polarization in the P(VDF-TrFE) films. We sequentially applied external voltage ranging from 0 V to +8 V with an interval of 2 V to the films. As the poling voltage increased, the initial d_{33} value of the firstly measured hysteresis loops at differently poled regions gradually increased and then reached a saturation at the poling voltage of +6 V (Fig. 3(d) and (e)). We confirmed that the degree of polarization alignment to the surface normal increased as the poling voltage increased. It should be noted that the initial d_{33} value with respect to the poling voltage is proportional to the amount of aligned polarization in the films. In addition, we calculated a volume fraction of oriented polarization perpendicular to the surface through eqn (1). The percentage of the relative ratio for the aligned polarization per unit volume beneath the AFM tip is defined as

$$P_{oriented} = d_{33,int}/d_{33,rem} \times 100 \qquad (1)$$

where $d_{33,int}$ is the initial d_{33} value obtained from the firstly measured hysteresis loop and $d_{33,rem}$ is the remnant d_{33} value obtained from the secondly measured hysteresis loop. The amount of the downward polarization formed by poling voltages of +2 V, +4 V, +6 V and +8 V were 14.3%, 36.5%, 97.3% and 100%, respectively.

Lastly, the effect of bottom electrode materials on self-polarization in the P(VDF-TrFE) film was investigated. Fig. 4 shows local piezoelectric hysteresis loops of the P(VDF-TrFE) films on both ITO and PEDOT:PSS electrodes. At the virgin state, the initial d_{33} value of the P(VDF-TrFE)/PEDOT:PSS stack (3.2 ± 1.2 pm V^{-1}) was much higher than that of the P(VDF-TrFE)/ITO stack (0.6 ± 2.1 pm V^{-1}). This coincides with PFM amplitude results shown in Fig. 1. In Fig. 4(b), the P(VDF-TrFE)/PEDOT:PSS stack showed higher remnant d_{33} (17.2 ± 1.8 pm V^{-1} vs. 15 ± 2.4 pm V^{-1}) and lower coercive voltage V_c (2.3 ± 0.3 V vs. 3.2 ± 0.6 V) than the P(VDF-TrFE)/ITO stack. The relative portion of the self-polarization in P(VDF-TrFE) films on ITO and PEDOT:PSS electrodes were 4% and 18.6%, respectively. Interestingly, we also found that the secondly measured hysteresis loop of the P(VDF-TrFE)/PEDOT:PSS stack was more positively shifted along the voltage axis (1.1 V vs. 0.7 V) as well as the d_{33} axis (1.7 pm V^{-1} vs. 0.3 pm V^{-1}) than that of the P(VDF-TrFE)/ITO stack. Generally, this hysteresis loop shift along the voltage axis can be elucidated by the work function (Φ) difference between top and bottom electrodes. Work function values of all materials used in
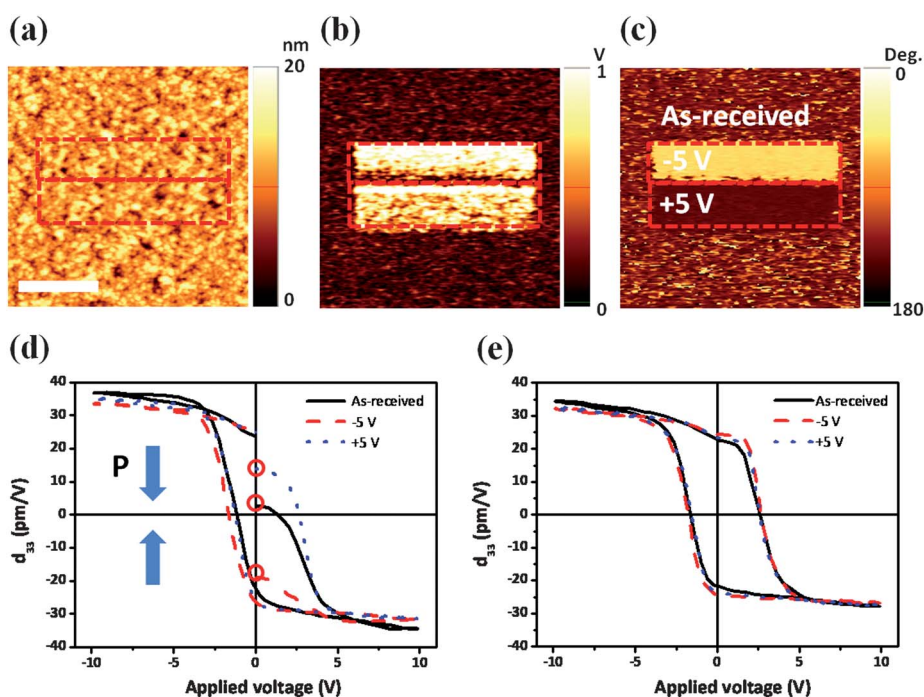
Fig. 2 (a) Topography, (b) PFM amplitude and (c) PFM phase images of three different regions (virgin state, poling of −5 V and poling of +5 V) in the P(VDF-TrFE) thin films on Au/Si substrates. (d) Firstly measured hysteresis loops at each regions. Red circles represent the initial points of the loops. (e) Secondly measured hysteresis loops at the same points with (d). 5 hysteresis loops were measured at different positions and averaged. The scale bar represents 1 μm.

this study are summarized in Table 2.[23–26] However, the work function difference between Pt and ITO electrodes is higher than that between Pt and PEDOT:PSS electrodes. This is opposite to the result shown in Fig. 4(b). Consequently, we confirmed that PEDOT:PSS would have stronger effect on self-polarization in the P(VDF-TrFE) film than ITO.
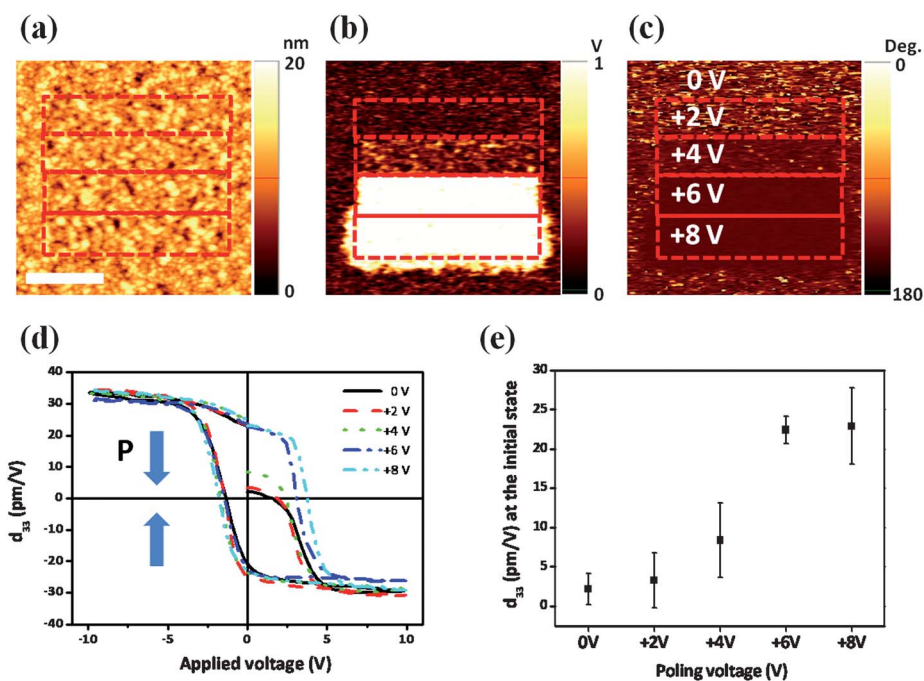
Fig. 3 (a) Topography, (b) PFM amplitude and (c) PFM phase images of the regions poled with various voltages from 0 V to +8 V with an interval of 2 V in the P(VDF-TrFE) thin films on Au/Si substrates. (d) Firstly measured hysteresis loops at each regions. (e) Initial d_{33} values depending on poling voltage. 5 hysteresis loops of each case were measured at different positions and averaged. The scale bar represents 1 μm.
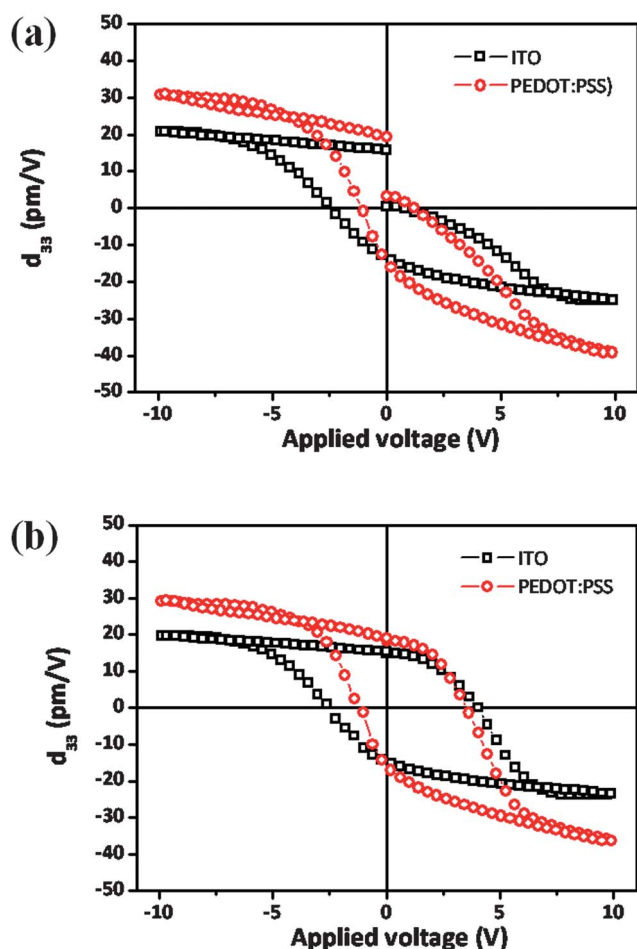
Fig. 4 (a) Firstly measured hysteresis loops and (b) secondly measured hysteresis loops of the P(VDF-TrFE) thin films on ITO and PEDOT:PSS electrodes. 10 hysteresis loops of each case were measured at different positions and averaged.

Although self-polarization in inorganic ferroelectric thin films has been reported by many researchers, its reason still remains unclear.[27–31] Unfortunately, this phenomenon has received scant attention in the field of ferroelectric polymers. Possible mechanisms in the inorganic ferroelectric thin films can be summarized as follows. The first possibility is the presence of a built-in-field due to the Schottky barrier between a bottom electrode and a ferroelectric film. The internal bias field related to the interface between the bottom electrode and the ferroelectric film may make electric dipoles aligned. In particular, the built-in field has an influence on the dipoles in the vicinity of the bottom electrode. The second possibility is the presence of a mechanical stress gradient imposed by a rigid substrate. The internal biaxial stress makes the unit cell of ferroelectric crystals become a truncated

pyramid (*i.e.* Ti[+4] ion is moved to the larger base of the deformed PbTiO$_3$ unit cell).[31] Unlike inorganic materials, ferroelectric polymers consist of amorphous and one (or more) crystalline phases in which polymer chains are differently packed. Their polarization reversal results from the rotation of molecules about their chain axes. The self-polarization due to the stress gradient cannot be neglected but the assessment is beyond the scope of this article. Accordingly, we think that our observation would be intimately linked with the built-in-voltage between the bottom electrode and the P(VDF-TrFE) layer. P(VDF-TrFE) ultrathin films would have the characteristic of an n-type semiconductor.[32] In an ideal metal–semiconductor (n-type) contact, the built-in-voltage V_{bi} is readily deduced to be[33]

$$qV_{bi} = [\Phi_M - \Phi_S] \tag{2}$$

where Φ_M is metal work function, Φ_S is semiconductor work function and q is the magnitude of the electronic charge. If $\Phi_M > \Phi_S$, there is a depletion of electrons in the semiconductor adjacent to the MS interface and thus positive charge of P(VDF-TrFE) copolymers needs to be piled up near interface. It should be noted that the built-in-voltage across the PEDOT:PSS-P(VDF-TrFE) contact is greater than that across the ITO-P(VDF-TrFE) contact. As a consequence, the built-in-voltage due to the Schottky barrier in the MS contact results in the self-polarization in the P(VDF-TrFE) ultrathin film. This also directs electric dipoles from the surface to the bottom electrode. Obviously, the degree of the self-polarization depends on the work function difference between the bottom electrode and the ferroelectric layer. Moreover, it is believed that the crystallinity and chain conformation of the ferroelectric films can be improved by the use of conductive polymer electrodes instead of metals and conductive oxides.[8,10,11,17] This improvement would give better adhesion and wetting during spin-coating, better acting as nucleation sites during crystallization and less chemical reaction at the interface due to aggressive fluorine atom in P(VDF-TrFE) copolymers.

Conclusions

We have demonstrated a PFM investigation about self-polarization in spin-coated P(VDF-TrFE) ultrathin films on different bottom electrodes, such as PEDOT:PSS and ITO. We determined the degree of their self-polarization by measuring the initial d_{33} values from the first measured piezoresponse hysteresis loops. Importantly, the P(VDF-TrFE) film coated on the PEDOT:PSS electrode showed stronger self-polarization alignment than that coated on the ITO electrode (18.6% *vs.* 4%). This would be elucidated by the built-in-voltage due to the Schottky barrier in the MS contact and the enhancement of crystallinity and chain conformation due to the strong coherence between P

Table 2 Work function values of all materials used in this study[a]

Pt	Au	PEDOT:PSS	ITO	P(VDF-TrFE)
5.12~5.93 eV[23]	5.1~5.47 eV[23]	4.7~5.4 eV[25]	4.4–4.5 eV[24]	4.0 eV[26]

[a] Note: Work function can change for crystalline orientation and surface treatment.

(VDF-TrFE) and PEDOT:PSS. We believe that the control of self-polarization alignment will be very useful for avoiding subsequent poling procedures to align electric dipoles through ferroelectric media. Currently, we are exploring the effect of residual stress on the self-polarization phenomena in the ferroelectric ultrathin film.

Acknowledgements

Notes and references

1 J. Li, S. I. Seok, B. Chu, F. Dogan, Q. Zhang and Q. Wang, *Adv. Mater.*, 2009, **21**, 217.
2 G. W. Taylor, J. R. Burns, S. M. Kammann, W. B. Powers and T. R. Welsh, *IEEE J. Oceanic Eng.*, 2001, **26**, 539.
3 J. Granstrom, J. Feenstra, H. A. Sodano and K. Farinholt, *Smart Mater. Struct.*, 2007, **16**, 1810.
4 V. V. Kochervinskii, *Crystallogr. Rep.*, 2003, **48**, 649.
5 M. Poulsen and S. Ducharme, *IEEE Trans. Dielectr. Electr. Insul.*, 2010, **17**, 1028.
6 B. Xu, Y. Ovchenkov, M. Bai, A. N. Caruso, A. V. Sorokin, S. Ducharme, B. Doudin and P. A. Dowben, *Appl. Phys. Lett.*, 2002, **81**, 4281.
7 L. Cai, H. Qu, C. Lu, S. Ducharme, P. A. Dowben and J. Zhang, *Phys. Rev. B: Condens. Matter Mater. Phys.*, 2004, **70**, 155411.
8 R. C. G. Naber, P. W. M. Blom, A. W. Marsman and D. M. de Leeuw, *Appl. Phys. Lett.*, 2004, **85**, 2032.
9 H. Xu, J. Zhong, X. Liu and J. Chen, *Appl. Phys. Lett.*, 2007, **90**, 092903.
10 H. Xu, X. Liu, X. Fang, H. Xie, G. Li, X. Meng, J. Sun and J. Chu, *J. Appl. Phys.*, 2009, **105**, 034107.
11 H. J. Jung, J. Chang, Y. J. Park, S. J. Kang, B. Lotz, J. Huh and C. Park, *Macromolecules*, 2009, **42**, 4148.
12 D. Y. Kusuma, C. A. Nguyen and P. S. Lee, *J. Phys. Chem. B*, 2010, **114**, 13289.
13 B. J. Rodriguez, S. Jesse, S. V. Kalinin, J. Kim, S. Ducharme and V. M. Fridkin, *Appl. Phys. Lett.*, 2007, **90**, 122904.
14 B. J. Rodriguez, S. Jesse, J. Kim, S. Ducharme and S. V. Kalinin, *Appl. Phys. Lett.*, 2008, **92**, 232903.
15 Y. Kim, W. Kim, H. Choi, S. Hong, H. Ko, H. Lee and K. No, *Appl. Phys. Lett.*, 2010, **96**, 012908.
16 Y. Y. Choi, J. Hong, S. Hong, H. Song, D.-S. Cheong and K. No, *Phys. Status Solidi RRL*, 2010, **4**, 94.
17 Y. Y. Choi, J. Hong, D.-S. Leem, M. Park, H. W. Song, T.-H. Sung and K. No, *J. Mater. Chem.*, 2011, **21**, 2057.
18 P. Sharma, T. J. Reece, S. Ducharme and A. Gruverman, *Nano Lett.*, 2011, **11**, 1970.
19 S. R. Forrest, *Nature*, 2004, **428**, 911.
20 J. A. Rogers, T. Someya and Y. Huang, *Science*, 2010, **327**, 1603.
21 T. M. Brown, J. S. Kim, R. H. Friend, F. Cacialli, R. Daik and W. J. Feast, *Appl. Phys. Lett.*, 1999, **75**, 1679.
22 S.-I. Na, S.-S. Kim, J. Jo and D.-Y. Kim, *Adv. Mater.*, 2008, **20**, 4061.
23 *CRC Handbook of Chemistry and Physics*, 2008, 12.
24 Y. Park, V. Choong, Y. Gao, B. R. Hsieh and C. W. Tang, *Appl. Phys. Lett.*, 1996, **68**, 2699.
25 A. M. Mardes, M. Kemerink, M. M. de Kok, E. Vinken, K. Maturova and R. A. J. Janssen, *Org. Electron.*, 2008, **9**, 727.
26 D. K. Davies, *Br. J. Appl. Phys.*, 1978, **2**, 345.
27 S. Sun, L. Liu and P. A. Fuierer, *Ferroelectrics*, 1994, **152**, 187.
28 A. L. Kholkin, K. G. Brooks, D. V. Talyor, S. Hiboux and N. Setter, *Integr. Ferroelectr.*, 1998, **22**, 525.
29 S. Sun, Y. Wang, P. A. Fuirer and B. A. Tuttle, *Integr. Ferroelectr.*, 1999, **23**, 25.
30 G. Suchaneck, T. Sandner, A. Deyneka, G. Gerlach and L. Jastrabik, *Ferroelectrics*, 2004, **298**, 309.
31 J. Kim, S. Hong, S. Buehlmann, Y. Kim, M. Park, Y. K. Kim and K. No, *J. Appl. Phys.*, 2010, **107**, 104112.
32 J. Choi, P. A. Dowben, S. Pebley, A. V. Bune and S. Ducharme, *Phys. Rev. Lett.*, 1998, **80**, 1328.
33 R. F. Pierret, *Semiconductor Device Fundamentals*, 1996, 477.